HHS Public Access

Author manuscript

Arterioscler Thromb Vasc Biol. Author manuscript; available in PMC 2024 May 01.

Published in final edited form as:

Arterioscler Thromb Vasc Biol. 2023 May ; 43(5): 674–683. doi:10.1161/ATVBAHA.122.318894.

ISGylation of NF-κBp65 by SCF^{FBXL19} E3 ligase diminishes endothelial inflammation

Lian Li[1,*], **Jiaxing Miao**[1,*], **Nargis Shaheen**[1], **Sarah J. Taleb**[1], **Jian Hu**[2], **Qinmao Ye**[1], **Jinshan He**[1], **Jiasheng Yan**[1], **Rama K. Mallampalli**[2], **Jing Zhao**[1,2,¶], **Yutong Zhao**[1,2,¶]

[1]Department of Physiology and Cell Biology, Dorothy M. Davis Heart and Lung Research Institute, the Ohio State University, Columbus, OH

[2]Department of Internal Medicine, the Ohio State University, Columbus, OH

Abstract

Background: Nuclear transcriptional factor κB (NF-κB) plays a pivotal role in endothelial cell (EC) inflammation. Protein ISGylation is regulated by E3 ISG15 ligases, however, ISGylation of NF-κBp65 and its role in EC functions have not been investigated. Here we investigate if p65 is ISGylated and the role of its ISGylation in endothelial functions.

Methods: In vitro ISGylation assay and EC inflammation were performed. EC specific transgenic mice were utilized in a murine model of acute lung injury.

Results: We find that NF-κBp65 is ISGylated in resting ECs and that the post-translational modification is reversible. TNFα and endotoxin stimulation of EC reduce p65 ISGylation, promoting its serine phosphorylation through reducing its association with a phosphatase WIP1. Mechanistically, a Skp1-Cul1-F-box-protein (SCF) E3 ligase, SCF^{FBXL19}, is identified as a new ISG15 E3 ligase that targets and catalyzes ISGylation of p65. Depletion of FBXL19 increases p65 phosphorylation and EC inflammation, suggesting a negative correlation between p65 ISGylation and phosphorylation. Moreover, EC specific hFBXL19 overexpressing humanized transgenic mice exhibit reduced lung inflammation and severity of experimental acute lung injury.

Conclusions: Together, our data reveal a new post-translational modification of p65 catalyzed by a previously unrecognized role of SCF^{FBXL19} as an ISG15 E3 ligase that modulates EC inflammation.

[¶]Address correspondence to: Yutong Zhao, MD, PhD, Department of Physiology and Cell Biology, The Ohio State University, 333 10th Avenue, Graves Hall 2166E, Columbus, OH, United States, 43210, Tel: 614-685-0036, yutong.zhao@osumc.edu, Jing Zhao, MD, PhD, Department of Physiology and Cell Biology, The Ohio State University, 333 10th Avenue, Graves Hall 2166D, Columbus, OH, United States, 43210, Tel: 614-685-0827, jing.zhao@osumc.edu.

[*]L. Li and J. Miao contributed equally.

Disclosures

The authors declare no conflict of interest related to this work.

Supplemental Material

Supplemental figures S1–S2

Major Resources Table

Keywords

ISG15; ISGylation; NF-κB; Post-translational modification; SCF E3 ligase; endothelial inflammation

Introduction

Microvascular endothelial dysfunction is a hallmark of acute inflammatory diseases, including acute lung injury and sepsis [1–4]. In response to stimuli, endothelial cells (ECs) release pro-inflammatory chemokines, including IL-6 and IL-8, to recruit neutrophil influx into inflamed regions. Endothelial dysfunction is associated with COVID-19 severity [5, 6]. Activated lung ECs increase intercellular adhesion molecule 1 (ICAM1) and vascular cell adhesion molecule 1 (VCAM1) expression on the EC surface to facilitate neutrophil adhesion and transmigration into interstitial lung tissues and alveolar spaces [7–11]. NF-κB, a transcriptional factor, has long been considered a master regulator of prototypical inflammatory signaling. p65 is the major subunit of NF-κB. In resting cells, p65 is associated with I-κB, forming an inactive complex. Upon stimulation, I-κB becomes phosphorylated and degraded, thus freeing p65 to translocate into the nucleus to trigger gene expression [12–15]. p65 transcriptional activation is regulated by its post-translational modifications (PTMs). Phosphorylation of p65 by IKKβ exhibits a profound effect on NF-κB activation [16–18], while the phosphorylation can be reversed by phosphatase WIP1 [19, 20].

Protein ISGylation is a newly characterized PTM [21–23]. It was initially found in IFN-γ signaling. ISG15, a ubiquitin-like protein, exhibits antiviral activity [24–26]. It is covalently conjugated to hundreds of proteins by a three-step enzymatic cascade including E1, E2, and E3 ligases. E3 ligases are key enzymes in ISGylation. So far, only a few ISG15 E3 ligases have been identified [22, 27–29]. ISGylation is a reversible process and de-ISGylation is mediated by USP18 (previously named as UBP43) [30, 31]. The functional consequences of ISGylation are largely unexplored even though it has been shown to regulate protein-protein interaction, enzyme activity, and protein translation. Recent studies indicate that ISG15 regulates TRAF6/TAK1, IKKβ, NEMO protein levels and p65 mRNA expression [32–36]; however, ISGylation of NF-κBp65 and the role of protein ISGylation in EC inflammation have not been reported.

The Skp1-cullin 1-F-box (SCF) ligase complex, one of the largest families of E3 ubiquitin ligases, is comprised of a substrate-recognition component termed the F-box protein [37, 38]. In this study, we characterize SCF^{FBXL19}-mediated ISGylation of NF-κBp65 and determined its role in the attenuation of p65 phosphorylation, EC inflammation, and lung injury. The data will lay the foundation for a significant mechanistic advance regarding the molecular regulation of the NF-κB pathway through the modulation of FBXL19 abundance and p65 ISGylation, which is implicated in the pathogenesis of inflammatory disorders such as acute lung injury and sepsis.

Materials and Methods

All data and study materials that support the findings of this study are available from the corresponding authors upon reasonable request.

Cells and reagents.

Human lung microvascular endothelial cells (HLMVECs, from ATCC) were cultured with endothelial growth medium-2 (EGM-2) containing antibiotics at 37°C in 5% CO_2. Human hybridoma endothelial cells (EAhy 926, ATCC) and HEK293 cells (from ATCC) were cultured in DMEM medium containing 10% fetal bovine serum (FBS). V5 tag antibody, mammalian expressional plasmid pcDNA3.1/His-V5-topo, and *Escherichia coli* Top10 competent cells were purchased from Life technologies (Grand Island, NY). ISG15, p65, ubiquitin, and WIP1 antibodies were purchased from Cell Signaling (Danvers, MA). ICAM1 and VCAM1 antibodies, immobilized protein A/G beads, and control IgG were purchased from Santa Cruz Biotechnology (Santa Cruz, CA). FBXL19 antibody was from Abgent (San Diego, CA). Lipopolysaccharide (LPS), T7 tag, and β-actin antibodies were purchased from Sigma (St. Louis, MO). Human recombinant TNFα was purchased from R&D systems (Minneapolis, MN). All materials used in the experiments are the highest grade commercially available.

Plasmid and siRNA transfection.

Human *USP18*, human *FBXL19*, or human *ISG15* cDNA were inserted into pCDNA3.1/V5-His-Topo vector, pCDNA3.1/HA vector. Human p65-T7 plasmid was a gift from Warner Greene (Addgene plasmid #21984). Plasmids and siRNAs transfections in ECs were performed using LipoJet or PepMute siRNA transfection reagent (SignaGen Laboratories, Frederick, MD). Overexpression or downregulation of genes were confirmed by immunoblotting.

Immunoblotting and co-immunoprecipitation (co-IP).

Cells were lysed in lysis buffer (Cell signaling, Danvers, MA). Equal amounts of total protein were subjected to SDS-PAGE gel, transferred to nitrocellulose, and then immunoreacted with primary and secondary antibody, sequentially. In figure legends, n indicates number of independent experiments. Membranes were stripped after phospho-p65 immunoblotting and then re-probed with anti-p65 antibody. For co-IP, 1 μg of protein was incubated with a primary antibody overnight at 4°C, followed by incubation with protein A/G beads for an additional 2 h in room temperature. The beads were rinsed with PBS and lysis buffer for 3 times. Proteins on the beads were eluted by boiling in 2x SDS sample buffer.

In vitro ISGylation assay.

Cell pellets were resuspended with ubiquitin aldehyde and N-ethylmaleimide in 50–80 μl of 2% SDS lysis buffer, followed by heating at 100°C for 10 min. This procedure disrupts any non-covalent protein-protein interaction. The denatured cell lysates were then sonicated on ice, followed by 10 times dilution with TBS. Cell lysates were subjected to IP.

Immunofluorescence staining.

EAHy 926 cells were cultured in glass-bottom dishes and fixed with 3.7% formaldehyde for 20 min. Cells were blocked by 1% BSA in TBST buffer, and then cells were exposed to primary antibodies, followed by incubation with fluorescence-labeled secondary antibodies. All the antibodies have been evaluated with species' IgGs as negative controls. Immunofluorescent cell imaging was performed using a Nikon A1R confocal microscope.

Animals and flow cytometry.

EC-specific FBXL19 overexpressing mice were generated by breeding endothelial cell-specific Cre transgenic mice (Tg(Tek-cre^{1Ywa}), from Jackson Laboratory Stock No. 008863) and human FBXL19-V5-2A-tdTomato knock-in-Loxp mice (FBXL19-KI$^{fl/fl}$, from Biocytogen Boston Corp, Wakefield, MA). Primers for genotyping are shown in supplemental figure 1. All mice were housed in the specific pathogen-free animal care facility at the Ohio State University in accordance with institutional guidelines and guidelines of the US National Institutes of Health. Standard laboratory rodent diet (5001* from LabDiet), containing ground corn, dehulled soybean meal, dried plain beet pulp, etc., was provided by animal care facility. All animal experiments were approved by the Ohio State University Animal Resources Centers. Age-matched males and females of C57/BL6J and EC-specific FBXL19 knock-in mice (8–10 weeks, 11 mice /each group, males and females) were given intratracheal (i.t.) LPS (2 mg/kg body weight) for 24 h. BAL fluid was collected for protein assay, cytospin, and neutrophil accounting. Lung tissues were fixed for hematoxylin and eosin (H&E) staining. Lung Evans blue staining were performed by intravenous injection of Evans blue in the mouse lateral tail vein, followed by lung collection and Evans blue measurement. Randomization and blinded analysis for data analysis were performed. Mice were randomly divided into two groups: the control group treated with PBS, the experimental lung injury group treated with i.t. LPS. Histological and BAL analysis were conducted by two independent investigators who are blinded to the samples. Data from males and females were combined for analysis. Lung tissues in C57/BL6J and EC-specific FBXL19 knock-in mice were minced and incubated in dissociation medium containing collagenase and DNase I at 37°C for 20 min. The digested lung tissue mixture was filtered with 70 μm nylon mesh strainer to obtain single cell suspension. FBXL19 expression in lung cell types were analyzed with flow cytometry with antibodies specific to FBXL19 and cell type markers. PerCP/Caynine5.5 anti-mouse CD326, APC anti-mouse CD45 antibody, and PE/Cyanine7 anti-mouse CD31 antibody were from BioLegend (San Diego, CA). FBXL19 antibody was labeled with FITC. The gating strategy (from negative to positive) was used to identify populations expressing endothelial cell surface maker CD31 (CD45−/CD326−/CD31+), epithelial cell marker CD326 (CD45−/CD31−/C326+), and leucocyte marker CD45 (CD326−/CD31−/CD45+).

Statistical analysis.

Statistical analysis was performed using GraphPad Prism software, version 8.0 (GraphPad Software, San Diego). Animal sample size estimation was based on previous results in comparable studies [39, 40]. A statistical power analysis was performed by employing G*Power 3.1.7 (Free software from Heinrich-Heine University, Germany) with assuming

90% power at a significance level of 0.05. Total 9–11 mice were used and data were pooled from two independent experiments. Biological sample size is indicated in the figure legends and data are expressed as means ± SEM. For continuous variables, normality and homogeneity of variance were assessed by Shapiro-Wilk and Brown-Forsythe tests, respectively. After confirming homogeneous variances and normality, 2-group comparisons for means were performed by 2-sided unpaired Student's t tests, and multiple group comparisons for means were performed by 2-way ANOVA with Bonferroni post hoc tests. P value of < 0.05 was considered significant.

Results

NF-κBp65 is ISGylated, which is reduced in response to inflammatory stimuli.

NF-κBp65 is a central transcriptional factor in innate immune responses. Several PTMs of NF-κBp65 have been shown to regulate p65 activation, including phosphorylation, acetylation, and ubiquitination [41]; however, ISGylation of NF-κBp65 has not described. To investigate whether p65 is ISGylated, we performed an *in vitro* ISGylation assay. Denatured EAhy926 cell lysates were subjected to IP with an antibody against p65, followed by immunoblotting with an ISG15 antibody. Mono-ISGylation of p65 was detected. ISGylation of p65 was reduced in *ISG15* siRNA-transfected cells (Fig. 1A), indicating that p65 can be ISGylated. USP18 is an ISG15 specific isopeptidase. p65 ISGylation was reduced in USP18-overexpressing EC cells (Fig. 1B), suggesting that p65 is ISGylated and that the PTM is reversed by USP18. Tumor necrosis factor α (TNFα) and endotoxin of gram-negative bacteria (lipopolysaccharide, LPS) trigger inflammatory responses in various inflammatory diseases through activation of NF-κB. Serine 536 phosphorylation of p65 is associated with NF-κB activation [41]. As shown in Fig. 1C, TNFα increased serine 536 phosphorylation of p65, whereas TNFα treatment of ECs reduced p65 ISGylation. Also, LPS treatment decreased p65 ISGylation in HLMVECs (Fig. 1D). To investigate if USP18 directly de-ISGylates p65, we performed co-immunoprecipitation (Co-IP) with a p65 antibody, followed by USP18 immunoblotting. As shown in Fig. 1E, USP18 was associated with p65 after LPS treatment, suggesting that LPS-reduced p65 ISGylation may occur through enhanced the association between p65 and USP18. Lysine (K) residues are protein ISGylation sites. To identify potential ISGylation sites on p65, we substituted several K of p65 with arginine (R). In vitro ISGylation assay showed that p65K218R, K221R, and K310R mutants reduced ISGylation levels (Fig. 1F), suggesting that these lysine residues are potential ISGylation sites. Taken together, these studies reveal that p65 can be ISGylated, a process reversed by USP18; inflammatory stimulus reduces p65 ISGylation, a process that may occur through increases in USP18/p65 association.

ISGylation regulates p65 phosphorylation and inflammatory responses.

To further investigate the relationship between ISGylation and phosphorylation of p65, we transfected ISG15 or USP18 plasmid in HLMVECs prior to TNFα treatment. TNFα induced serine 536 phosphorylation of p65, while the effect was attenuated by ISG15 overexpression and augmented by USP18 overexpression (Fig. 2A–D), suggesting that ISGylation impedes p65 phosphorylation. Upregulation of ICAM1 is a hallmark of EC inflammation, which is tightly regulated by NF-κB activation [42]. Overexpression of

ISG15 attenuated TNFα-induced ICAM1 expression (Fig. 2E, 2F). Further, we found that compared to the effect of p65 wild type, p65K310R increased TNFα-induced ICAM1 levels (Fig. 2G, 2H), suggesting that ISGylation negatively regulates p65 phosphorylation and inflammatory responses in ECs. Serine 536 phosphorylation of p65 is reversed by WIP1 [19]. To further investigate the molecular mechanisms by which ISGylation negatively regulates p65 phosphorylation, the association of p65 with WIP1 was examined by Co-IP. As shown in Fig. 3, overexpression of ISG15-V5 enhances p65 association with WIP1, suggesting that ISGylation of p65 compromises its phosphorylation through enhancing p65 association with its phosphatase.

SCF^{FBXL19} E3 ligase targets p65 for its ISGylation.

SCF^{FBXL19} is an anti-inflammatory E3 ligase and its leucine-rich repeat (LRR) region is responsible for interacting with substrates [38, 43]. Here we found that exogenously expressed FBXL19 wild type, but not the LRR deletion mutant of FBXL19 (FBXL19C300), increased ISGylation of p65 (Fig. 4A). Downregulation of FBXL19 by siRNA transfection decreased p65 ISGylation (Fig. 4B). Further, co-IP and co-immunofluorescence staining show that FBXL19 is associated with p65 (Fig. 4C, 4D), indicating that SCF^{FBXL19} is an ISG15 E3 ligase for p65 in ECs (Fig. 4E).

SCF^{FBXL19} E3 ligase attenuates p65 phosphorylation and EC inflammation.

Next, we examined the effect of SCF^{FBXL19} on phosphorylation of p65, which regulates p65 transcriptional activity. As shown in Fig. 5A and 5B, downregulation of FBXL19 by siRNA transfection significantly increased phosphorylation of p65, indicating that FBXL19 regulates p65 ISGylation while attenuating p65 phosphorylation. NF-κB activation determines EC inflammation. Overexpression of FBXL19-V5 reduces TNFα-induced ICAM1 and VCAM1 expression in HLMVECs (Fig. 5C–E), while downregulation of FBXL19 promotes ICAM1 and VCAM1 expression (Fig. 5F, 5G). To determine the impact of SCF^{FBXL19} on leukocyte adhesion to EC, we examined the adhesion of GFP-expressing THP1 (human monocytic cell line) cells to TNFα-treated control cells or FBXL19-knockdown or overexpressing HLMVECs. *FBXL19* siRNA transfected HLMVECs showed increased THP1 adhesion (Fig. 5H, 5I), while FBXL19-overexpressing HLMVECs exhibited lower inflammatory activity evidenced by lower levels of THP1 adhesion (Fig. 5J, 5K). These data suggest that SCF^{FBXL19} diminishes EC inflammation, in part, through mediating p65 ISGylation and activation.

EC-specific FBXL19 overexpression reduces lung inflammation.

To further investigate the role of EC-FBXL19 in lung inflammation, we generated EC-specific FBXL19 overexpression mice. An $FBXL19^{fl/fl}$ mouse strain (C57BL/6J background) was generated by inserting the CAG-loxP/STOP/loxP-hFBXL19-V5 with 2A-tdTomato marker cassette into the Rosa26 locus, in the intron between endogenous exon 1 and 2. Further, the mice were crossed with Tek-Cre mice to generate EC specific V5-tagged human FBXL19-overexpressing mice (Tek-Cre/FBXL19-$KI^{fl/fl}$) (Fig. 6A). The expression of FBXL19-V5 was detected in lung lysates (Fig. 6B) and CD31 positive ECs in Tek-Cre/FBXL19-$KI^{fl/fl}$ mice (supplemental Fig. 2). tdTamoto positive signal was detected in CD31 positive ECs by immunofluorescence staining (Fig. 6C). Mouse lung

single cell suspensions were isolated. Isolated ECs showed tdTomato positive (Fig. 6D). FBXL19 levels were increased in ECs ($CD31^+/CD45^-/CD326^-$), but not in epithelial cells ($CD326^+/CD31^-/CD45^-$) and leukocytes ($CD45^+/CD31^-/CD326^-$), from Tek-Cre/FBXL19-$KI^{fl/fl}$ mouse lungs compared with cells from $FBXL19^{fl/fl}$ mouse lungs (Fig. 6E). To determine if overexpression of FBXL19 in ECs diminishes EC inflammation in a murine model of acute lung injury (ALI), we challenged Tek-Cre/FBXL19-$KI^{fl/fl}$ (FBXL19-KI) and $FBXL19^{fl/fl}$ (WT control) with intratracheal (i.t.) injection of LPS (2 mg/kg body weight, 24 h). Bronchoalveolar lavage (BAL) fluid was collected and analyzed for neutrophil influx into lungs. As shown in Fig. 7A and 7B, LPS injection increased neutrophil influx into the lungs of WT mice, which was significantly reduced in FBXL19-KI mice. H&E staining of lung tissues indicated that LPS-induced immune cell infiltration was decreased in FBXL19-KI mice (Fig. 7C). Further, pulmonary microvascular leakage was determined by the Evans blue (EB) technique in lung tissues. Compared to the lungs from LPS-challenged WT mice, EB content was decreased in the lungs of LPS-challenged FBXL19-KI mice (Fig. 7D, 7E). Protein levels in BAL fluid were also reduced in LPS-challenged FBXL19-KI mice, compared to LPS-challenged WT mice (Fig. 7F), indicating that overexpression of FBXL19 in ECs diminishes microvascular dysfunction in response to LPS challenge.

Discussion

ISG15 is a ubiquitin-like protein induced by interferons. ISGylation is the conjugation of ISG15 to substrate proteins. Antiviral effects of ISGylation have been well studied [23, 24, 26, 28]. Recent studies suggest that ISGylation plays an anti-inflammatory role in bacterial infection [34, 44]. NF-κB activation contributes to inflammatory responses including chemokine, ICAM1, and VCAM1 production in ECs [43]. NF-κBp65 undergoes several PTMs that regulate p65 stability, localization, and transcriptional activation [41]. The effect of ISGylation on NF-κB activation has been reported [32–34, 36]; however, the ISGylation of p65 has not been identified. This study reveals that p65 can be ISGylated and that the ISGylation is regulated by E3 ligase SCF^{FBXL19} and de-ISGylation enzyme USP18. p65 ISGylation is reduced in response to inflammatory stimuli, such as LPS and TNFα, leading to an increase of its phosphorylation and inflammatory responses in ECs. Further, we show that EC-specific overexpression of FBXL19 diminishes lung inflammation in a murine model of acute lung injury. This study is the first to identify the ISGylation of p65 and provide a new molecular mechanism underlying regulation of NF-κB activation.

ISGylation is mediated by E1 activating enzyme (Ube1L), E2 conjugating enzyme (UbcH8), and an E3 ligase [28]. Several E3 ligases including HERC5, Trim25, and human homologue of Ariadne (HHARI) have been identified to modulate ISGylation [27, 29, 45, 46]. SCF E3 ligase family belongs to multi-subunit RING-finger type of E3 ligase, which contains a cul1, Skp1, and F-box protein. Among them, the F-box protein is responsible for interaction with substrates [37, 38]. The role of SCF E3 ligases in protein ubiquitination and neddylation has been well studied; however, its role in ISGylation has not been reported. We show that SCF^{FBXL19} targets and induces ISGylation of p65, while USP18 reverses the ISGylation. The p65 ISGylation is confirmed by downregulation of ISG15. Deletion of LRR domain of FBXL19 failed to induce p65 ISGylation, suggesting that specific molecular signatures are indispensable for SCF^{FBXL19} mediated ISG15 E3 ligase activity for p65. It is possible

that the LRR domain is a p65 docking site within FBXL19. SCF^{FBXL19} exhibits an anti-inflammatory property through targeting and ubiquitinating the IL-33 receptor and CBP histone acetyltransferase [47, 48]. This study reveals a new target for SCF^{FBXL19}. UbcH8 also serves as E2 enzyme for ubiquitin in SCF E3 ligase-mediated ubiquitination system [49]. UbcH8 has been shown to regulate both ubiquitination and ISGylation of the RNA helicase retinoic inducible gene 1 (RIG-1) [50]. We hypothesize that UbcH8 plays a role as an E2 enzyme in SCF^{FBXL19}-mediated p65 ISGylation. Future studies will be performed to investigate the complex of Ube1L/UbcH8/ SCF^{FBXL19}. It is possible that other E3 ligases may induce p65 ISGylation. HERC5 levels have been shown be upregulated by LPS in ECs [51]; however, its role in LPS-induced inflammatory responses have not been investigated. we will further identify additional E3 ligases for p65 ISGylation in the future studies.

NF-κBp65 phosphorylation is associated with its transcriptional activation. Interplay between different PTMs regulate NF-κB activation as p65 phosphorylation promotes its acetylation and transcriptional activation [41]. ISGylation occurs on lysine residues of substrates and the molecular ISGylation site remains elusive. Further, the phosphorylated state of p65 is functionally relevant, is reversible, and controlled in part by the phosphatase WIP1 that reduces NF-κB activation [20]. Our data show that ISGylation promotes WIP1 association with p65. This may explain why ISGylation is associated with lower p65 phosphorylation. Additionally, it is possible that ISGylation may induce p65 conformational changes to prevent phosphatase conjugation to p65. We show that serine 536 phosphorylation of p65 is altered by ISGylation. P65 can be phosphorylated in several serine or threonine sites. Whether ISGylation affects this phosphorylation also needs additional studies. In this study, we demonstrate that TNFα and LPS regulate p65 ISGylation. It is possible that other inflammatory stimuli may affect p65 ISGylation. Activation of p65 regulates inflammatory responses in other lung cells, such as macrophages and epithelial cells. In this study, we focused on endothelial cells, but p65 ISGylation may also occur in other cell types. A small number of hematopoietic cells are reported to be Cre positive in Tek-cre^{1Ywa} allele [52]. There is possible that FBXL19 overexpression in blood cells may contribute to the anti-inflammatory effects in Tek-Cre-FBXL19KI mice.

In summary, this study is the first to unveil p65 ISGylation, mediated by SCF^{FBXL19}, and reversed by USP18 in ECs that impacts inflammation. ISGylation of p65 reduces EC inflammation, suggesting that SCF^{FBXL19}-mediated p65 ISGylation exhibits an anti-inflammatory property in ECs. Reduction of ISGylation by inflammatory stimuli promotes p65 phosphorylation and EC inflammation (Fig. 8). The data opens new opportunities to investigate NF-κB activation in inflammatory diseases to better understand the signatures that regulate of p65 ISGylation through molecular interplay with other modifications that govern cell-specific behavior.

Supplementary Material

Refer to Web version on PubMed Central for supplementary material.

Sources of Funding

This research was supported by National Institutes of Health, R01HL131665, R01HL136294, and R01HL157164 to Y.Z., R01GM115389 and R01HL151513 to J.Z. and P01 HL114453, R01 HL081784, and R01HL097376 to R.K.M. All the authors have read the journal's authorship agreement and that the manuscript has been reviewed by and approved by all named authors.

Nonstandard Abbreviations

NF-κB	Nuclear transcriptional factor κB
EC	endothelial cell
SCF	Skp1-Cul1-F-box-protein
ICAM1	intercellular adhesion molecule 1
VCAM1	vascular cell adhesion molecule 1
PTM	post-translational modifications
IP	immunoprecipitation
WT	wild type
EB	Evans blue
i.t	intratracheal
HHARI	human homologue of Ariadne
RIG-1	retinoic inducible gene 1

References

1. Cines DB, Pollak ES, Buck CA, Loscalzo J, Zimmerman GA, McEver RP, Pober JS, Wick TM, Konkle BA, Schwartz BS, Barnathan ES, McCrae KR, Hug BA, Schmidt AM and Stern DM. Endothelial cells in physiology and in the pathophysiology of vascular disorders. Blood. 1998;91:3527–61. [PubMed: 9572988]
2. Oude Nijhuis CS, Vellenga E, Daenen SM, Kamps WA and De Bont ES. Endothelial cells are main producers of interleukin 8 through Toll-like receptor 2 and 4 signaling during bacterial infection in leukopenic cancer patients. Clin Diagn Lab Immunol. 2003;10:558–63. [PubMed: 12853386]
3. Xiao L, Liu Y and Wang N. New paradigms in inflammatory signaling in vascular endothelial cells. Am J Physiol Heart Circ Physiol. 2014;306:H317–25. [PubMed: 24285111]
4. Zhao H, Anand AR and Ganju RK. Slit2-Robo4 pathway modulates lipopolysaccharide-induced endothelial inflammation and its expression is dysregulated during endotoxemia. J Immunol. 2014;192:385–93. [PubMed: 24272999]
5. Siddiqi HK, Libby P and Ridker PM. COVID-19 - A vascular disease. Trends Cardiovasc Med. 2021;31:1–5. [PubMed: 33068723]
6. Zhang J, Tecson KM and McCullough PA. Endothelial dysfunction contributes to COVID-19-associated vascular inflammation and coagulopathy. Rev Cardiovasc Med. 2020;21:315–319. [PubMed: 33070537]
7. Li L, Wei J, Mallampalli RK, Zhao Y and Zhao J. TRIM21 mitigates human lung microvascular endothelial cells inflammatory responses to lipopolysaccharide. Am J Respir Cell Mol Biol. 2019.

8. Zhao Y, Gorshkova IA, Berdyshev E, He D, Fu P, Ma W, Su Y, Usatyuk PV, Pendyala S, Oskouian B, Saba JD, Garcia JG and Natarajan V. Protection of LPS-induced murine acute lung injury by sphingosine-1-phosphate lyase suppression. Am J Respir Cell Mol Biol. 2011;45:426–35. [PubMed: 21148740]
9. Nonas S, Miller I, Kawkitinarong K, Chatchavalvanich S, Gorshkova I, Bochkov VN, Leitinger N, Natarajan V, Garcia JG and Birukov KG. Oxidized phospholipids reduce vascular leak and inflammation in rat model of acute lung injury. Am J Respir Crit Care Med. 2006;173:1130–8. [PubMed: 16514111]
10. Huang X, Dai Z, Cai L, Sun K, Cho J, Albertine KH, Malik AB, Schraufnagel DE and Zhao YY. Endothelial p110gammaPI3K Mediates Endothelial Regeneration and Vascular Repair After Inflammatory Vascular Injury. Circulation. 2016;133:1093–103. [PubMed: 26839042]
11. Ohmura T, Tian Y, Sarich N, Ke Y, Meliton A, Shah AS, Andreasson K, Birukov KG and Birukova AA. Regulation of lung endothelial permeability and inflammatory responses by prostaglandin A2: role of EP4 receptor. Mol Biol Cell. 2017;28:1622–1635. [PubMed: 28428256]
12. Ahmed AU, Sarvestani ST, Gantier MP, Williams BR and Hannigan GE. Integrin-linked kinase modulates lipopolysaccharide- and Helicobacter pylori-induced nuclear factor kappaB-activated tumor necrosis factor-alpha production via regulation of p65 serine 536 phosphorylation. J Biol Chem. 2014;289:27776–93. [PubMed: 25100717]
13. Gross CM, Kellner M, Wang T, Lu Q, Sun X, Zemskov EA, Noonepalle S, Kangath A, Kumar S, Gonzalez-Garay M, Desai AA, Aggarwal S, Gorshkov B, Klinger C, Verin AD, Catravas JD, Jacobson JR, Yuan JX, Rafikov R, Garcia JGN and Black SM. LPS-induced Acute Lung Injury Involves NF-kappaB-mediated Downregulation of SOX18. Am J Respir Cell Mol Biol. 2018;58:614–624. [PubMed: 29115856]
14. Hayden MS and Ghosh S. Regulation of NF-kappaB by TNF family cytokines. Semin Immunol. 2014;26:253–66. [PubMed: 24958609]
15. Sehnert B, Burkhardt H, Wessels JT, Schroder A, May MJ, Vestweber D, Zwerina J, Warnatz K, Nimmerjahn F, Schett G, Dubel S and Voll RE. NF-kappaB inhibitor targeted to activated endothelium demonstrates a critical role of endothelial NF-kappaB in immune-mediated diseases. Proc Natl Acad Sci U S A. 2013;110:16556–61. [PubMed: 24062461]
16. Schutze S, Wiegmann K, Machleidt T and Kronke M. TNF-induced activation of NF-kappa B. Immunobiology. 1995;193:193–203. [PubMed: 8530143]
17. Karin M The beginning of the end: IkappaB kinase (IKK) and NF-kappaB activation. J Biol Chem. 1999;274:27339–42. [PubMed: 10488062]
18. Li ZW, Chu W, Hu Y, Delhase M, Deerinck T, Ellisman M, Johnson R and Karin M. The IKKbeta subunit of IkappaB kinase (IKK) is essential for nuclear factor kappaB activation and prevention of apoptosis. J Exp Med. 1999;189:1839–45. [PubMed: 10359587]
19. Salminen A and Kaarniranta K. Control of p53 and NF-kappaB signaling by WIP1 and MIF: role in cellular senescence and organismal aging. Cell Signal. 2011;23:747–52. [PubMed: 20940041]
20. Chew J, Biswas S, Shreeram S, Humaidi M, Wong ET, Dhillion MK, Teo H, Hazra A, Fang CC, Lopez-Collazo E, Bulavin DV and Tergaonkar V. WIP1 phosphatase is a negative regulator of NF-kappaB signalling. Nat Cell Biol. 2009;11:659–66. [PubMed: 19377466]
21. Malakhov MP, Kim KI, Malakhova OA, Jacobs BS, Borden EC and Zhang DE. High-throughput immunoblotting. Ubiquitiin-like protein ISG15 modifies key regulators of signal transduction. J Biol Chem. 2003;278:16608–13. [PubMed: 12582176]
22. Ubiquitylation Staub O. and isgylation: overlapping enzymatic cascades do the job. Sci STKE. 2004;2004:pe43.
23. Hermann M and Bogunovic D. ISG15: In Sickness and in Health. Trends Immunol. 2017;38:79–93. [PubMed: 27887993]
24. Perng YC and Lenschow DJ. ISG15 in antiviral immunity and beyond. Nat Rev Microbiol. 2018;16:423–439. [PubMed: 29769653]
25. Morales DJ and Lenschow DJ. The antiviral activities of ISG15. J Mol Biol. 2013;425:4995–5008. [PubMed: 24095857]
26. Jeon YJ, Yoo HM and Chung CH. ISG15 and immune diseases. Biochim Biophys Acta. 2010;1802:485–96. [PubMed: 20153823]

27. Mathieu NA, Paparisto E, Barr SD and Spratt DE. HERC5 and the ISGylation Pathway: Critical Modulators of the Antiviral Immune Response. Viruses. 2021;13. [PubMed: 35062217]
28. Giannakopoulos NV, Arutyunova E, Lai C, Lenschow DJ, Haas AL and Virgin HW. ISG15 Arg151 and the ISG15-conjugating enzyme UbE1L are important for innate immune control of Sindbis virus. J Virol. 2009;83:1602–10. [PubMed: 19073728]
29. Nakasato N, Ikeda K, Urano T, Horie-Inoue K, Takeda S and Inoue S. A ubiquitin E3 ligase Efp is up-regulated by interferons and conjugated with ISG15. Biochem Biophys Res Commun. 2006;351:540–6. [PubMed: 17069755]
30. Malakhov MP, Malakhova OA, Kim KI, Ritchie KJ and Zhang DE. UBP43 (USP18) specifically removes ISG15 from conjugated proteins. J Biol Chem. 2002;277:9976–81. [PubMed: 11788588]
31. Ritchie KJ, Hahn CS, Kim KI, Yan M, Rosario D, Li L, de la Torre JC and Zhang DE. Role of ISG15 protease UBP43 (USP18) in innate immunity to viral infection. Nat Med. 2004;10:1374–8. [PubMed: 15531891]
32. Minakawa M, Sone T, Takeuchi T and Yokosawa H. Regulation of the nuclear factor (NF)-kappaB pathway by ISGylation. Biol Pharm Bull. 2008;31:2223–7. [PubMed: 19043203]
33. Yang Z, Xian H, Hu J, Tian S, Qin Y, Wang RF and Cui J. USP18 negatively regulates NF-kappaB signaling by targeting TAK1 and NEMO for deubiquitination through distinct mechanisms. Sci Rep. 2015;5:12738. [PubMed: 26240016]
34. Xiao J, Li S, Zhang R, Wang Z, Zhang X, Wang A, Jin Y and Lin P. ISGylation Inhibits an LPS-Induced Inflammatory Response via the TLR4/NF-kappaB Signaling Pathway in Goat Endometrial Epithelial Cells. Animals (Basel). 2021;11. [PubMed: 35011117]
35. Adapala NS, Swarnkar G, Arra M, Shen J, Mbalaviele G, Ke K and Abu-Amer Y. Inflammatory osteolysis is regulated by site-specific ISGylation of the scaffold protein NEMO. Elife. 2020;9.
36. Mao H, Wang M, Cao B, Zhou H, Zhang Z and Mao X. Interferon-stimulated gene 15 induces cancer cell death by suppressing the NF-kappaB signaling pathway. Oncotarget. 2016;7:70143–70151. [PubMed: 27659523]
37. Skaar JR, Pagan JK and Pagano M. SCF ubiquitin ligase-targeted therapies. Nat Rev Drug Discov. 2014;13:889–903. [PubMed: 25394868]
38. Kipreos ET and Pagano M. The F-box protein family. Genome Biol. 2000;1:REVIEWS3002. [PubMed: 11178263]
39. Pouzol L, Sassi A, Baumlin N, Tunis M, Strasser DS, Lehembre F and Martinic MM. CXCR7 Antagonism Reduces Acute Lung Injury Pathogenesis. Front Pharmacol. 2021;12:748740. [PubMed: 34803691]
40. Chen IC, Wang SC, Chen YT, Tseng HH, Liu PL, Lin TC, Wu HE, Chen YR, Tseng YH, Hsu JH, Dai ZK, Suen JL and Li CY. Corylin Ameliorates LPS-Induced Acute Lung Injury via Suppressing the MAPKs and IL-6/STAT3 Signaling Pathways. Pharmaceuticals (Basel). 2021;14. [PubMed: 35056069]
41. Huang B, Yang XD, Lamb A and Chen LF. Posttranslational modifications of NF-kappaB: another layer of regulation for NF-kappaB signaling pathway. Cell Signal. 2010;22:1282–90. [PubMed: 20363318]
42. Kempe S, Kestler H, Lasar A and Wirth T. NF-kappaB controls the global pro-inflammatory response in endothelial cells: evidence for the regulation of a pro-atherogenic program. Nucleic Acids Res. 2005;33:5308–19. [PubMed: 16177180]
43. Jackson PK and Eldridge AG. The SCF ubiquitin ligase: an extended look. Mol Cell. 2002;9:923–5. [PubMed: 12049727]
44. Malakhova O, Malakhov M, Hetherington C and Zhang DE. Lipopolysaccharide activates the expression of ISG15-specific protease UBP43 via interferon regulatory factor 3. J Biol Chem. 2002;277:14703–11. [PubMed: 11854279]
45. Wong JJ, Pung YF, Sze NS and Chin KC. HERC5 is an IFN-induced HECT-type E3 protein ligase that mediates type I IFN-induced ISGylation of protein targets. Proc Natl Acad Sci U S A. 2006;103:10735–40. [PubMed: 16815975]
46. Lee JM, Choi SS, Lee YH, Khim KW, Yoon S, Kim BG, Nam D, Suh PG, Myung K and Choi JH. The E3 ubiquitin ligase TRIM25 regulates adipocyte differentiation via proteasome-mediated degradation of PPARgamma. Exp Mol Med. 2018;50:135. [PubMed: 30323259]

47. Zhao J, Wei J, Mialki RK, Mallampalli DF, Chen BB, Coon T, Zou C, Mallampalli RK and Zhao Y. F-box protein FBXL19-mediated ubiquitination and degradation of the receptor for IL-33 limits pulmonary inflammation. Nat Immunol. 2012;13:651–8. [PubMed: 22660580]

48. Wei J, Dong S, Yao K, Martinez M, Fleisher PR, Zhao Y, Ma H and Zhao J. Histone acetyltransferase CBP promotes function of SCF FBXL19 ubiquitin E3 ligase by acetylation and stabilization of its F-box protein subunit. FASEB J. 2018;32:4284–4292. [PubMed: 29522376]

49. Johansson P, Jeffery J, Al-Ejeh F, Schulz RB, Callen DF, Kumar R and Khanna KK. SCF-FBXO31 E3 ligase targets DNA replication factor Cdt1 for proteolysis in the G2 phase of cell cycle to prevent re-replication. J Biol Chem. 2014;289:18514–25. [PubMed: 24828503]

50. Arimoto K, Konishi H and Shimotohno K. UbcH8 regulates ubiquitin and ISG15 conjugation to RIG-I. Mol Immunol. 2008;45:1078–84. [PubMed: 17719635]

51. Kroismayr R, Baranyi U, Stehlik C, Dorfleutner A, Binder BR and Lipp J. HERC5, a HECT E3 ubiquitin ligase tightly regulated in LPS activated endothelial cells. J Cell Sci. 2004;117:4749–56. [PubMed: 15331633]

52. Payne S, De Val S and Neal A. Endothelial-Specific Cre Mouse Models. Arterioscler Thromb Vasc Biol. 2018;38:2550–2561. [PubMed: 30354251]

Highlights

- NF-κBp65 can be ISGylated by SCF^{FBXL19} E3 ligase, that can be reversed by USP18.
- ISGylation of p65 reduces its phosphorylation through increasing its association with phosphatase WIP1.
- Increases in p65 ISGylation diminish lung EC inflammation.
- Overexpression of FBXL19 in ECs reduces severity of experimental lung injury.

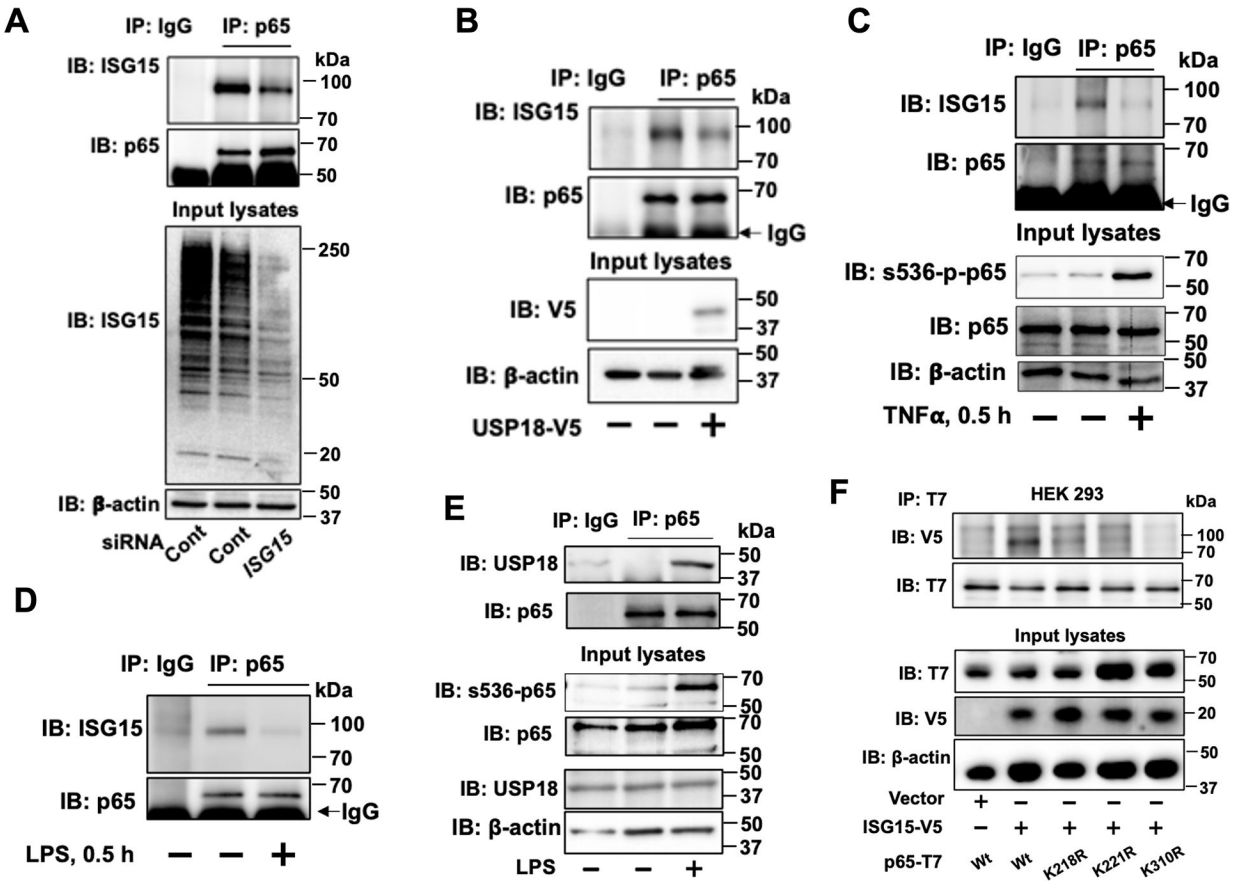

Figure 1. TNFα and LPS reduce p65 ISGylation in ECs.

A.,B. p65 ISGylation was examined in *ISG15* siRNA - **(A)** or USP18-V5- **(B)** transfected EAhy 926 cells. Input cell lysates were analyzed by antibodies for ISG15 **(A)** and V5 **(B). C.,D.** p65 ISGylation was examined in TNFα (5 ng/ml, 0.5 h)- **(C)** or LPS (100 ng/ml, 0.5 h) **(D)**-treated HLMVECs. Input lysates were analyzed by Ser536-p-p65 and p65 immunoblotting **(C)**. **E.** The association between p65 and USP18 in HLMVECs was examined by Co-IP. **F.** In vitro ISGylation of p65-T7 wild type (Wt), K218R, K221R, and K310R mutants was examined in HEK293 cells. Immunoblots are representatives of two independent experiments.

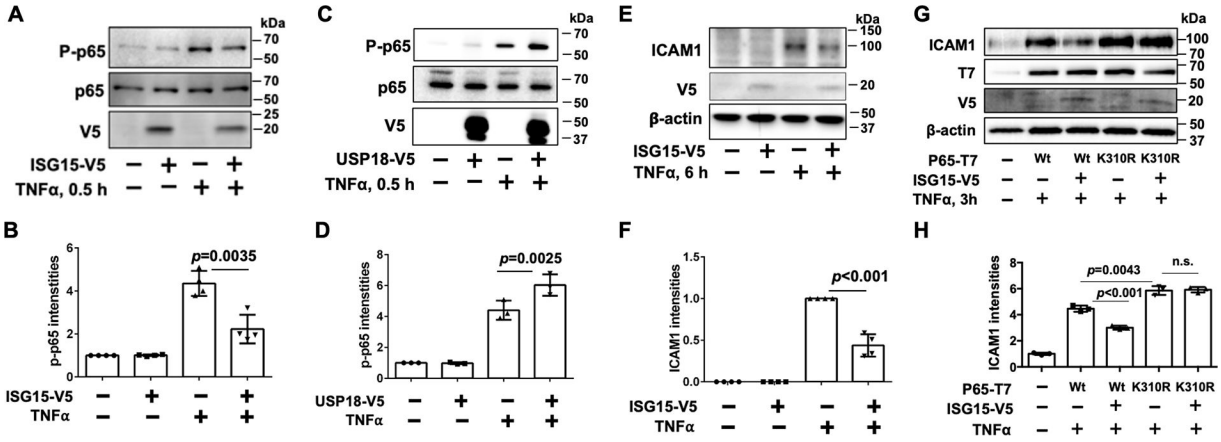

Figure 2. ISGylation regulates TNFα-induced phosphorylation of p65 and ICAM1 expression in HLMECs.

HLMVECs were transfected with ISG15-V5 **(A, E)** or USP18-V5 **(C)** plasmid for 48 h, followed by TNFα (5 ng/ml, 0.5 and 6 h) treatment. P-p-65 (**A, C**) and ICAM1 (**E**) levels were analyzed. P-p65/p65 (**B, D**) and ICAM1/β-actin (**F**) intensities were quantified by Image J. n=4 samples per group. **G.** HLMVECs were transfected with the indicated plasmids, followed by TNFα (5 ng/ml, 3 h) treatment. ICAM1 levels were analyzed and quantified by Image J (**H**). n=3 samples per group. Data are presented as the means ± SEM. 2-way ANOVA with Bonferroni post hoc tests were used. Immunoblots are representatives of three or four independent experiments.

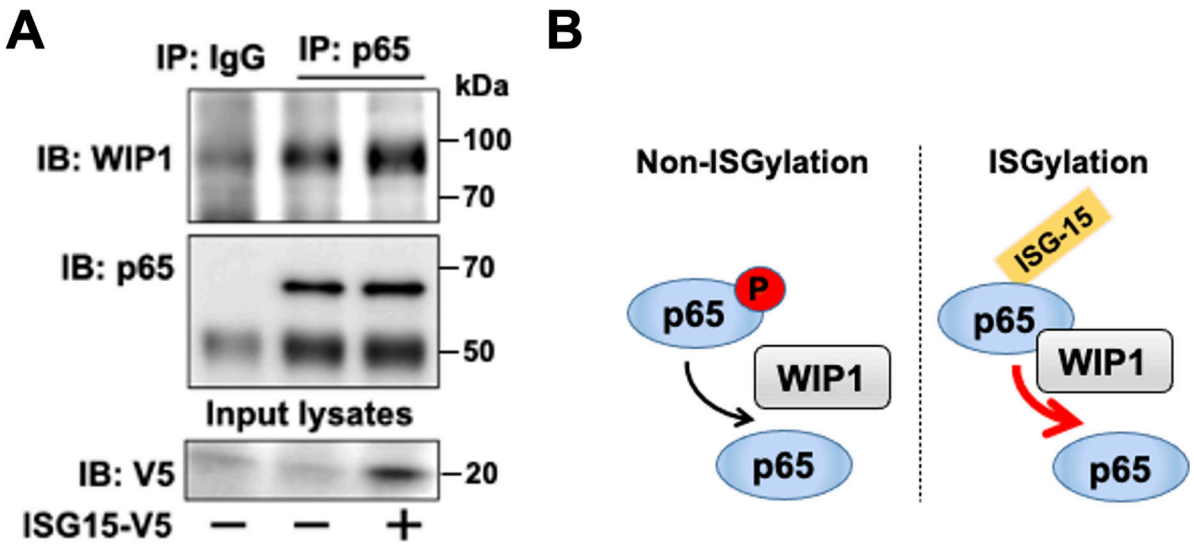

Figure 3. ISGylation increases p65 association with WIP1.

A. EAHy 926 cells were transfected with ISG15-V5 plasmid for 48 h. Cell lysates were subjected to IP with a p65 antibody, followed by immunoblotting with antibodies for WIP1 and p65. Immunoblots are representatives of two independent experiments. **B.** Scheme shows ISGylated p65 association with WIP1.

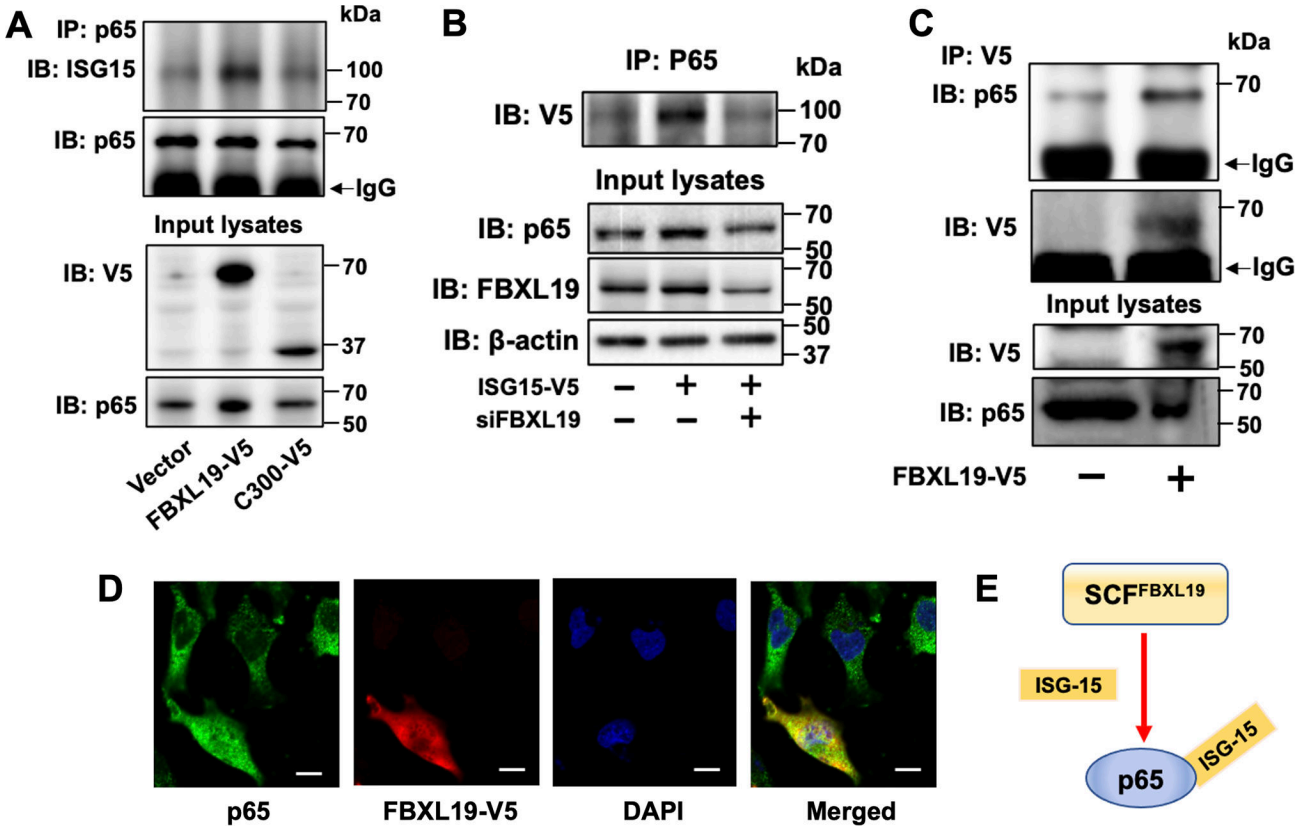

Figure 4. SCF^{FBXL19} E3 ligase targets p65 for its ISGylation.

A. EAhy 926 cells were transfected with FBXL19-V5 or FBXL19C300-V5 plasmid for 48 h. ISGylation of p65 was examined. **B.** HLMVECs were transfected with FBXL19 siRNA or ISG15-V5 for 72h. In vitro ISGylation were performed. **C.** EAhy 926 cells were transfected with FBXL19-V5 plasmid for 48 h. Cell lysates were subjected to IP with a V5 antibody, followed by immunoblotting with antibodies for p65 and V5. Immunoblots are representatives of two independent experiments. **D.** EAhy 926 cells were transfected with FBXL19-V5 plasmid for 24 h. Co-immunofluorescence staining were performed with V5 and p65 antibodies. Scale bar, 10 μm. **E.** Scheme shows that SCF^{FBXL19} induces p65 ISGylation.

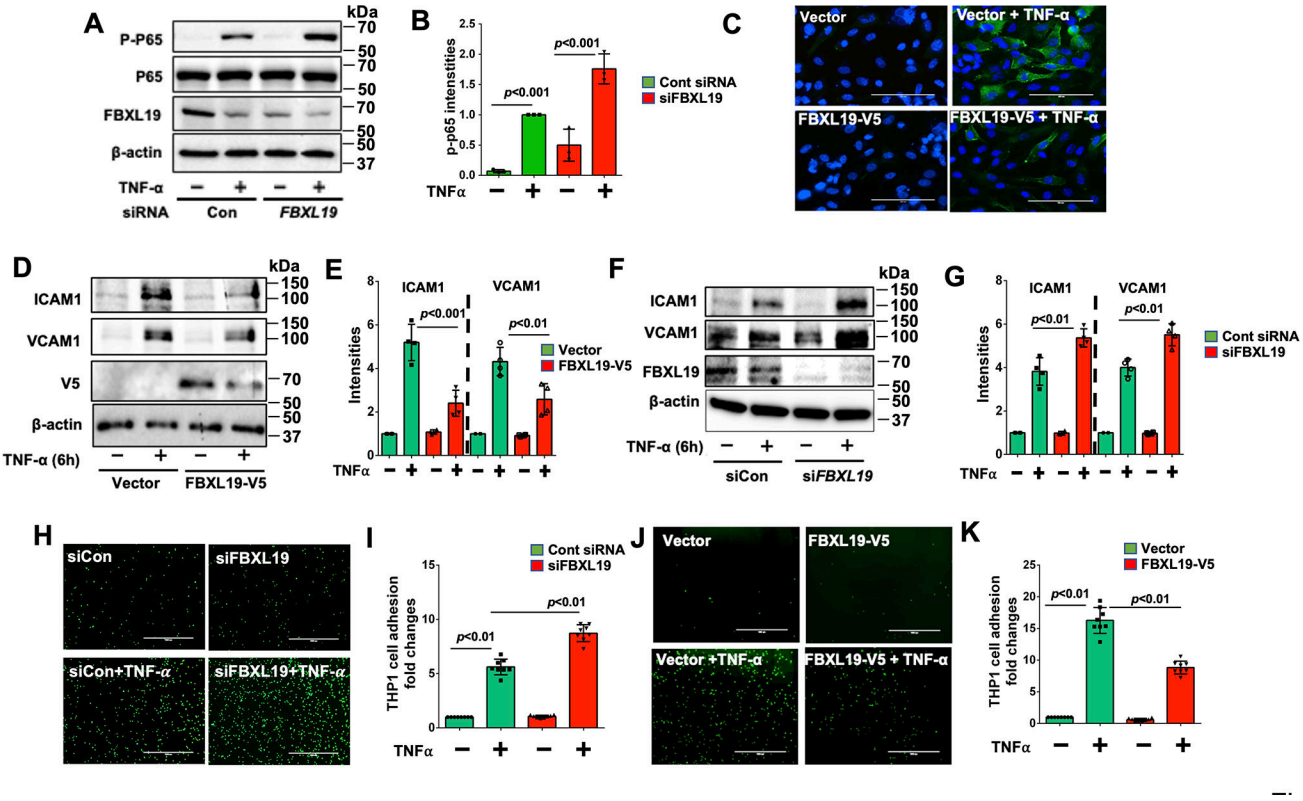

Figure 5. SCF^{FBXL19} diminishes p65 phosphorylation and HLMVEC inflammation.

A. HLMVECs were transfected with cont siRNA or *FBXL19* siRNA for 72 h and then treated with TNFα (5 ng/ml) for 0.5 h. p-p65 was examined and intensities of p-p65/p65 were quantified. n=3 samples per group **(B)**. **C.** ICAM1 immunofluorescence staining (green) after TNFα treatment (10 ng/ml, 6 h) in empty vector or FBXL19-V5 transfected HLMVECs. Scale bar, 50 μm. **D.,F.** ICAM1, VCAM1, V5, and FBXL19 immunoblotting after TNFα treatment (10 ng/ml, 6 h). Intensities of ICAM1/β-actin and VCAM1/β-actin were quantified. n=4 samples per group **(E, G). H., J.** *FBXL19* siRNA- or FBXL19-V5-transfected HLMVECs were treated with TNFα for 6 h, and then GFP-expressing THP1 cells were added. After 30 min, unattached THP1 were washed out. Immunofluorescence signals were measured and quantified. Scale bar, 50 μm. n=12 samples per group (**I.,K.**). Data are presented as the means ± SEM. 2-way ANOVA with Bonferroni post hoc tests were used. Immunoblots and images are representatives of three or four independent experiments.

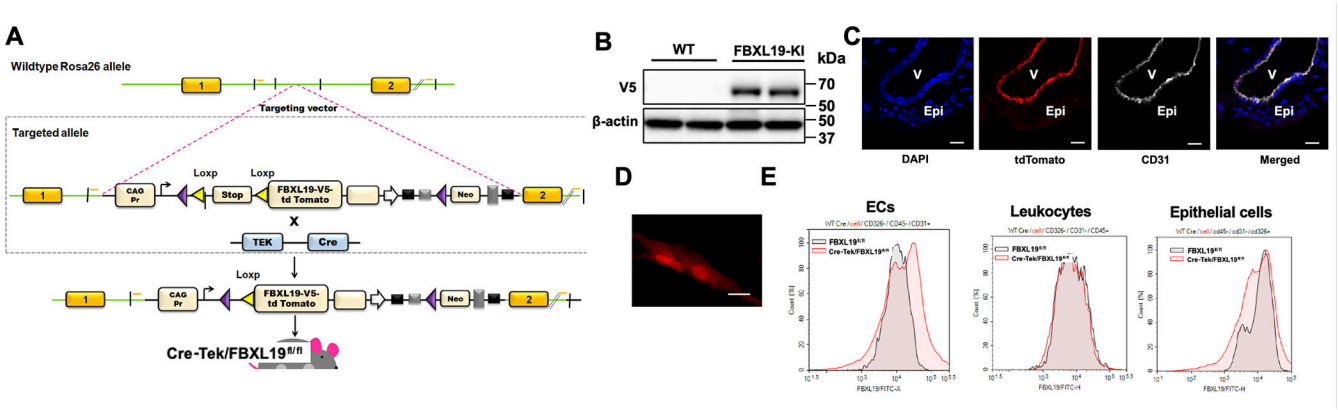

Figure 6. Generation of Tek-Cre/FBXL19-KI$^{fl/fl}$ (FBXL19-KI) mice.

A. Strategy of generation of Tek-Cre/FBXL19-KI$^{fl/fl}$ mice. **B.** Lung tissue lysates were analyzed by immunoblotting with a V5 antibody. **C.** tdTomato signals were localized in CD31 positive EC cells. v: vascular vessel; Epi: epithelium. Scale bar, 100 μm. **D.** tdTomato fluorescence imaging of isolated lung endothelial cells. Scale bar, 10 μm. **E.** FBXL19 expression in lung single cell suspensions was analyzed by flow cytometry. CD31^{+}/CD45^{-}/CD326^{-} (ECs), CD45^{+}/CD31^{-}/CD326^{-} (leukocytes), CD326^{+}/CD31^{-}/CD45^{-} (epithelial cells). Grey: FBXL19$^{fl/fl}$ control; Red: Tek-Cre/FBXL19-KI$^{fl/fl}$.

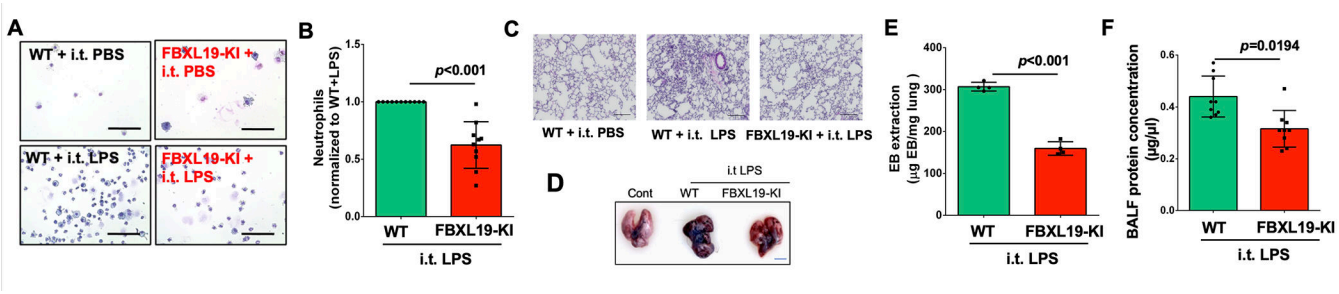

Figure 7. Tek-Cre/FBXL19-KI$^{fl/fl}$ mice exhibit reduced EC inflammation in a murine model of acute lung injury.

FBXL19-KI and FBXL19$^{fl/fl}$ (WT control) with i.t. injection of LPS (2 mg/kg body weight, 24 h). **A.** Cytospin images of neutrophil in BAL fluids. Scale bar, 150 μm. **B.** Neutrophil in BAL fluids were quantified. n=10–11. The numbers of mice were pooled from two independent experiments. P value was calculated by *t* test. **C.** H&E staining of lung tissues. Scale bar, 100 μm. **D.** Images of lung tissues stained with Evans Blue (EB). Scale bar, 0.5 cm. **E.** EB content in the lungs were quantified. n=4 mice / group. P value was calculated by *t* test (**F**). Protein levels in BAL fluids were measured. n=9 mice/group. The numbers of mice were pooled from two independent experiments. Data are presented as the means ± SEM. An unpaired Student *t* test was used.

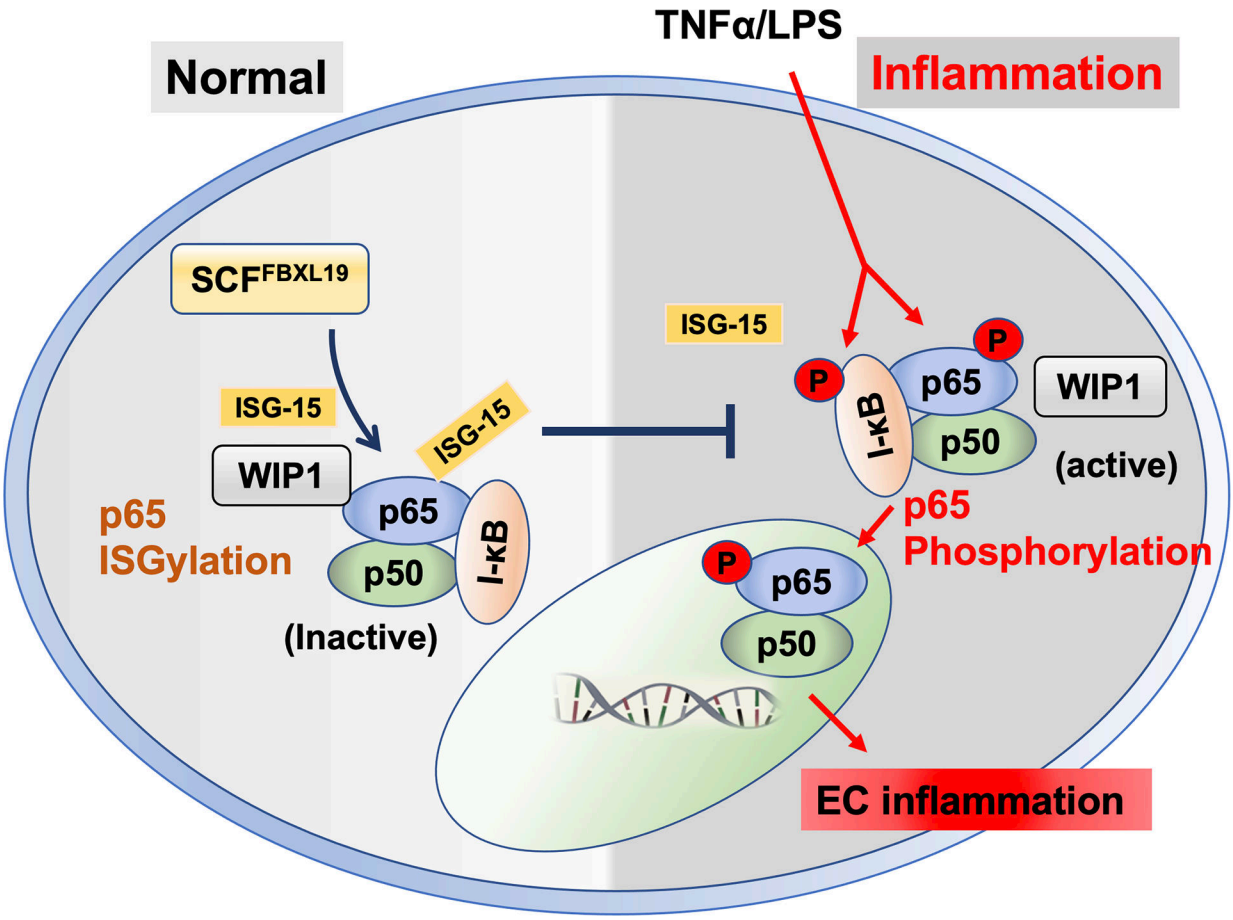

Figure 8. Scheme of SCF^{FBXL19}-mediated p65 ISGylation diminishes p65 phosphorylation and EC inflammation.